Comparison of Constant and Variable Fluid Properties with Variable Heat Flux over a Sheet for Maxwell Fluid

Javaria Aafaq Tarar
Regn.00000321345

A thesis submitted in partial fulfillment of the requirements
for the degree of **Master of Science**
in
Mathematics

Supervised by: Dr. Muhammad Asif Farooq

Department of Mathematics

School of Natural Sciences
National University of Sciences and Technology
H-12, Islamabad, Pakistan

Year 2019-2021

National University of Sciences & Technology

MS THESIS WORK

We hereby recommend that the dissertation prepared under our supervision by: JAVARIA AAFAQ TARAR, Regn No. 00000321345 Titled: Comparison of constant and variable fluid properties with variable heat flux over a sheet for Maxwell fluid be accepted in partial fulfillment of the requirements for the award of **MS** degree.

Examination Committee Members

1. Name: DR. MERAJ MUSTAFA HASHMI   Signature: _____

2. Name: DR. MUJEEB UR REHMAN   Signature: _____

External Examiner: DR. SHAFQAT HUSSAIN   Signature: _____

Supervisor's Name DR. M. ASIF FAROOQ   Signature: _____

_____
Head of Department

11/10/2021
Date

COUNTERSINGED

Date: 12·10·2021

_____
Dean/Principal

Dedication
This study is dedicated to my loving parents, supportive husband, and encouraging mother-in-law for their never ending love, prayers and support.

Acknowledgements

Abstract

A comparison of constant and variable fluid properties with variable heat flux over a sheet for Maxwell fluid is done in the presence of thermal radiation, magnetic parameter, and thermal conductivity. The governing partial differential equations (PDEs) are converted into a set of associated non-linear ordinary differential equations (ODEs), which are then explaine numerically using pertinent boundary conditions for distinct physical parameters by using *bvp4c* in MATLAB. On the velocity, temperature profiles, as well as the local skin-friction coefficient and the local Nusselt number, the effects of various parameters such as viscosity, thermal conductivity, unsteadiness, Deborah number, thermal radiation, magnetic parameter, and Darcy number are introduced and explained. The numerical results are compared to those previously published. The result show that for both constant and variable fluid properties skin friction coefficient escalate with the increase in magnetic parameter, unsteadiness parameter, Darcy number, thermal conductivity and Deborah number. Constant fluid properties are independent of heat generation/absortion parameter. For both cases local Nusselt number decreases with the increase in magnetic parameter, Deborah number, heat generation/absortion parameter and Darcy number.

Contents

List of Figures

List of Tables

Chapter 1

Introduction

1.1 Introduction

A substance which deforms under the pressure of shear stress is called a fluid. The study of fluids in motion or at rest, as well as it's effects on the boundaries, which can be solid surfaces or with other fluids is labelled as fluid mechanics. The interpretation of fluid in motion is known as fluid dynamics while the analysis of fluids at rest is tagged as fluid statics. Gases and liquids both fall in the category of fluids. The amount of fluid that passes through a point per unit time is called flow. The fluid flow across a stretching surface has previously attracted a lot of attention. This is due to its wide range of uses such as Plastic films, polymer extrusion, glass fibre etc. Because of its numerous uses in engineering, the non-Newtonian fluids flow across a stretching surface has gotten a lot of attention in recent decades. Chemical engineering, and polymer fluids, plastic and rubber sheet production, and solidification liquid crystals, hot rolling, and crystal growing are all its examples. Numerous astrophysical phenomena, astrionics, and engineering processes rely on fluid flow together with heat transfer methods with MHD applications [1, 2].

Investigating some of the underlying key processes that affect the heat transfer surface is one technique to improve the performance of heat mechanisms [3, 4]. The work [5-10] provides a generalisation for fluid flow models in the context of unsteady flow. The heat flux is another key factor that can have an impact on the heat process mechanism. As a result, a number of research [11-13] have been published on these

themes, demonstrating that the fluid flow, in combination with the heat flux, is critical in several industrial operations. Liu et al. [14] were the first to develop a variable heat flux framework that is compatible with unsteady fluid flow models under a variety of situations. Our understanding of the specific nature of heat transmission mechanisms, however, is still lacking. Non-Newtonian fluid modelling studies present exciting difficulties for engineers, numerical analyst, physicists, and IT worker. Rajagopal [15] investigated accurate explanation for a class of unsteady unidirectional fluid flows of a second-grade fluid in four flow scenarios. Furthermore, the consequences of stress relaxation are impossible to predict. The flow of a Newtonian fluid in a thin liquid film over an unstable stretched sheet was initially explored by Wang [16]. The Maxwell model, that contains a branch of rate-type fluids, has gained popularity because it may anticipate stress relaxation. Applying a similarity method to transform the presiding boundary layer equations into ordinary differential equations, some authors [17-20] investigated the problem of flow along with heat transfer for the Maxwell fluid above a stretching surface. Tan et al. [17] proposed the fractional calculus technique to the constitutive relationship model of a generalised Maxwell fluid. Hayat et al. [18] investigated the three-dimensional flow of a non-Newtonian Maxwell fluid caused by a stretching surface with convective boundary conditions.

Mukhopadhyay [19] investigates unsteady two-dimensional flow of an MHD non-Newtonian Maxwell fluid over a stretching surface with a specified surface temperature in the presence of a heat source/sink. Megahed et al.[21] explore the effect of unsteady laminar MHD flow over an unsteady stretched sheet in the company of thermal radiation and changing heat flux.[20] Megahad et al. [22] investigated the effects of variable fluid characteristics on laminar MHD Newtonian flow together with the heat transfer past an unsteady stretching sheet implanted in a porous medium, particularly when variable heat flux was present.

In the above mentioned studies no attention was given to the constant fluid properties. The goal of the present research is to elaborate a comprehensive comparison of constant and variable fluid properties with variable heat flux over a sheet for Maxwell fluid.

2

1.2   Types of Fluids

1.2.1   Compressible vs Incompressible Fluids

An incompressible fluid flow is the one in which density variations are negligible. All liquids are treated as incompressible fluids. On contrary, the fluid flows that are characterized by a varying density are said to be compressible. Most commonly encountered gases are compressible fluids. Continuity equations for compressible and incompressible flows are respectively:

$$\rho_t + \nabla.(\rho \mathbf{V}) = 0$$

and

$$\nabla.\mathbf{V} = 0$$

1.2.2   Ideal vs Real Fluids

Ideal flows are the incompressible and irrotational fluid flows. In such fluids, shearing force between the fluid and the bounding surface is absent. On the other hand, fluid flows involving viscosity or surface shearing forces are termed as real flows.

1.2.3   Steady vs Unsteady Fluid Flow

In steady flows, all the physical quantities (such as density, velocity, acceleration etc) do not vary with time. Mathematically, for any quantity χ one has:

$$\chi_t = 0$$

For unsteady flow, the physical quantities exhibit time dependency. Therefore,

$$\chi_t \neq 0$$

where χ is any physical quantity.

1.2.4 Laminar vs Turbulent Fluid Flow

Laminar flow is a kind of flow in which each fluid particle follows a definite path an streamlines do not cross each other. Turbulent flow, on the other hand, do not exhibit a regular pattern of flow that leads to the rapid changes in physical properties of the fluid. For example, the flows in a pipe at low speed and flow of water along the edges of river/lake, falls in laminar flows. When a dye drop is injected in water, it spreads in all possible directions without following any proper pattern, thereby making the flow turbulent.

1.2.5 Newtonian vs Non-Newtonian Fluid

Fluids are continuously deforming objects and behave differently subjected to an applied shear stress. The response of fluids under applied stress determines whether the fluids obey a linearly viscous model (also called as "Newton's law of viscosity") or a non-linear one. Although, linear viscous model is capable of explaining certain important concepts like skin-drag, lift phenomena and separation, etc. but it fails to predict certain physical phenomenon like rod-climbing, die-swelling, shear-thinning, shear-thickening and viscoelasticity to name a few. This inadequacy of Newton's law of viscosity to predict such anomalous behaviors serves as a stimulus for

researchers to work in the area. Fluids exhibiting such behaviors are termed non-Newtonian.

1.3 Boundary Layer flow

A thin layer surrounding the boundary, in which the viscosity effects are significant and important in determining the fluid flow, is known as boundary layer. It acts as a buffer region between the free stream region and the wall. All these flows that follow the boundary layer theory (proposed by Prandlt in 1904) are termed as boundary layer flows.
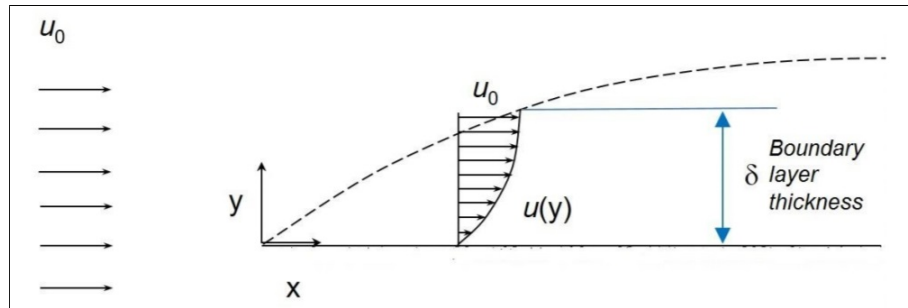
Figure 1.1: Boundary Layer Flow. (internet)

1.4 Dimensionless Parameters

1.4.1 Prandatl Number

It is the fraction of kinematic viscosity to thermal diffusivity. Numerically it is defined as:

$$\mathrm{Pr} = \frac{\nu}{\alpha},$$

where α is the thermal diffusivity that is further is defined as $\alpha = \frac{k}{\rho Cp}$ in which k represents thermal conductivity, ρ denotes density and Cp is specific heat capacity at constant pressure and ν is the kinematic viscosity.

1.4.2 Reynolds Number

It is the ratio of inertial force to the viscous force. Reynolds number allows us to differentiate whether the flow is laminar or turbulent. At low Re we have laminar

regime (i.e. Re $<$ 2000) and for high Reynolds number (Re $>$ 4000) we have turbulent regime. Mathematically,

$$\text{Re} = \frac{vL}{\nu},$$

where L is characteristic length, ν is kinematic velocity of the fluid and v is of fluid velocity.

1.4.3 Thermal Conductivity

The intrinsic property of a material which explains the materials capability to conduct heat is known as thermal conductivity i.e κ.

1.4.4 Nusselt Number

When there is a heat transfer from convection flow to conduction flow in fluids across the boundary. The heat transfer is perpendicular to surface of the boundary. Mathematically,

$$\text{Nu} = \frac{QL}{k},$$

where L is length of the disk/sheet, k is thermal conductivity of the fluid and Q is convective heat transfer coefficient.

1.5 *bvp4c*

Flows occurring in physical world are governed by complex non-linear partial differential equations. These equations may have no solution, or may have a finite number, or may have infinitely many solutions. In order to get a solution MATLAB programs require the user to provide with the initial guesses for the solution required and also for the parameters involved in the governing equations. MATLAB built in package *bvp4c*, which implements collocation method, is capable of solving a nonlinear boundary value problem. In order to utilize this technique, the third order equations are reduced to ordinary differential equations of first order. The guesses are provided for more accurate results. Changes can be made in step size to increase accuracy. To get more detailed understanding of this technique Refs. [23] and [24] can be consulted.

Chapter 2

Numerical Results for Newtonian Fluid Flow over an Unsteady Stretching Sheet with Variable Heat Flux

This chapter discusses flow over an unsteady stretching sheet in the presence of porous medium, variable heat flux and thermal radiation. In Section 2.1 we discuss the mathematical formulation of the flow model. In Section 2.2 the governing equations are solved numerically using *bvp4c* in MATLAB. In Section 2.3 the validation of proposed method is given, and finally in the Section 2.4, the results are described with the aid of graphs.

2.1 Mathematical Formulation

A laminar boundary layer flow is considered. The flow is viscous, incompressible and two dimensional. Heat transfer because of an unsteady stretching sheet is also considered. The physical properties such as fluid viscosity, thermal conductivity, and the surface velocity which are μ, κ and U_w, respectively. Variable heat flux $q^*(x,t)$ is also involved in this model i.e.

$$q^*(x,t) = -\kappa_{eff}\frac{\partial T}{\partial y} = T_0\frac{dx^r}{(1-at)^{m+\frac{1}{2}}}, \tag{1}$$

where

T_0= reference temperature,

a= positive constant,

d= constant,

r= space index,

m= time index,

And B is the transverse magnetic field can be interpolated as follows [25]:

$$B = \frac{B_0}{(1 - at)^{\frac{1}{2}}},$$ (2)

where B_0 is a constant. The physical phenomenon can be described by the following partial differential equations. Liu et al. [14]

$$u_x + v_y = 0,$$ (3)

$$u_t + uu_x + vu_y = \frac{1}{\rho_\infty}(\mu u_y)_y - \frac{\sigma B^2 u}{\rho_\infty} - \frac{\mu u}{\rho_\infty \kappa},$$ (4)

$$T_t + uT_x + vT_y = \frac{1}{\rho_\infty C_p}(\kappa T_y)_y - \frac{1}{\rho_\infty C_p}(q_r)_y,$$ (5)

where x and y are directions, while v and u are velocity components. Also t, ρ_∞, σ, k, T, C_p and q_r are the time, fluid density (away from sheet), electrical conductivity, porosity of porous medium, temperature of the fluid, specific heat at constant pressure and radiative heat flux respectively. Parsad et al. [26] introduced q_r in terms of T as:

$$q_r = -\frac{4\sigma^*}{3k^*}\frac{\partial T^4}{\partial y},$$ (6)

where k^* and σ^* are the Rosseland mean absorption coefficient and the Stefan-Boltzmann constant, respectively. Expanding T^4 about T into the Taylor series and neglecting higher order partial derivatives we get:

$$T^4 \approx 4T_\infty^3 T - 3T_\infty^4.$$

Boundary condition corresponding to considered model is taken as,

$$u = U_w, v = 0, -\kappa_{eff}T_y = q^*(x,t), \quad \text{at} \quad y = 0$$ (7)

$$u \to 0, T \to T_\infty \quad as \quad y \to \infty.$$ (8)

8

where

$$\kappa_{eff} = \kappa + \frac{16\sigma^* T_\infty^3}{3K^*}$$

T_∞ is the temperature of the fluid, and U_w is defined as

$$U_w = \frac{bx}{1 - at}. \tag{9}$$

The similarity variables are defined as, [22]:

$$\eta = \left(\frac{b}{\nu_\infty(1 - at)}\right)^{\frac{1}{2}} y, \tag{10}$$

$$\psi = (\nu_\infty b)^{\frac{1}{2}} x f(\eta),$$

$$\theta(\eta) = \frac{T - T_\infty}{\left(\frac{q(x,t)}{\kappa_\infty}\right)\sqrt{\frac{\nu_\infty}{b}}(1 - at)^{\frac{1}{2}}}, \tag{11}$$

where $\theta(\eta)$, and $f(\eta)$ are the dimensionless temperature and dimensionless velocity function respectively. Also $\psi(x,y)$ is the stream function and the kinematic velocity at ambient is ν_∞.

The fluid viscosity (μ) and thermal conductivity (ϵ) are the functions of temperature.

$$\frac{\mu}{\mu_\infty} = e^{-\alpha\theta}, \frac{\kappa}{\kappa_\infty} = (1 + \epsilon\theta), \tag{12}$$

where

$\mu_\infty =$ viscosity at the surrounding,

$\alpha =$ dimensionless viscosity,

$\kappa_\infty =$ thermal conductivity away from the surface,

$\epsilon =$ thermal conductivity.

Equation of continuity is satisfied by using similarity variables in Eq (10) and (11). And Eq (4) and (5) are as follow after converting partial differential equation into ordinary differential equation by using similarity variables

$$e^{-\alpha\theta}\left(f''' - \theta'\alpha f''\right) - Mf' - e^{-\alpha\theta}\gamma f' - S\left(f' + \frac{\eta}{2}f''\right) - f'^2 + ff'' = 0, \tag{13}$$

$$\frac{1}{Pr}\left[(1 + R + \epsilon\theta)\theta'' + \epsilon\theta'^2\right] - rf'\theta + f\theta' - S\left(\frac{\eta}{2}\theta' + m\theta\right) = 0, \tag{14}$$

9

and the converted boundary conditions are:

$$f(0) = 0, f'(0) = 1, \theta'(0) = -\frac{1}{1 + \epsilon\theta + R}, \tag{15}$$

$$f' \to 0, \qquad \theta \to 0 \quad as \quad \eta \to \infty. \tag{16}$$

Here R and ϵ are the thermal radiation parameter and the thermal conductivity parameter, respectively and heat flux depends on them. The parameter $R = \frac{16\sigma^* T_\infty^3}{3\kappa_\infty k*}$ is the radiation parameter, $M = \frac{\sigma B^2}{b\rho_\infty}$ is the magnetic field, $Pr = \frac{\mu_\infty C_p}{\kappa_\infty}$ is the Prandtl number, $\gamma = \frac{\mu_\infty(1-at)}{\rho_\infty kb}$ is the local Darcy number, $S = \frac{a}{b}$ is the unsteadiness parameter. In equation (13). and (14). temperature and velocity fields are coupled to each other. Crane [27] solved the velocity field systematically for steady problem $S = 0$, $R = 0$, $M = 0$, $\gamma = 0$ i.e when the thermal radiation, magnetic field and porous parameter are not present and $\alpha = 0$ i.e viscosity is not a function of temperature, with $f = 1 - e^{-\eta}$.
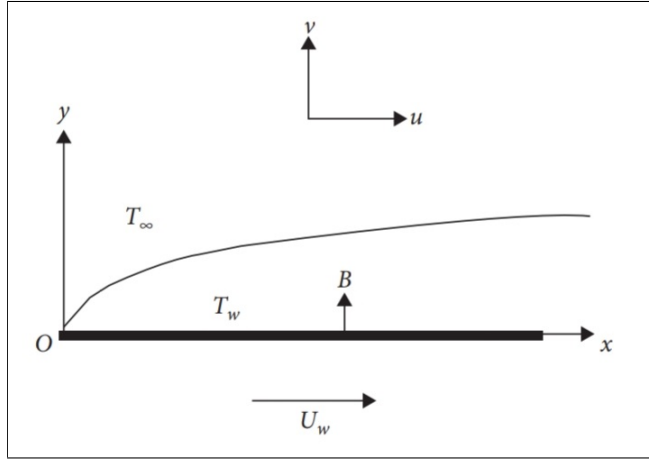
Figure 2.1: Physical model. [22]

2.2   Quantities of Interest

The dimensionless physical parameters are the skin friction and the local Nusselt number.

2.2.1 Skin Friction Coefficient

The skin friction coefficient is written as;

$$Cf_x Re_x^{\frac{1}{2}} = -2e^{\alpha\theta(0)} f''(0). \tag{17}$$

2.2.2 Local Nusselt Number

The local Nusselt number is defined as;

$$Nu_x Re_x^{\frac{1}{2}} = \frac{1}{\theta(0)}, \tag{18}$$

where the local Reynolds number is $Re = \frac{U_w x}{\nu_\infty}$.

2.3 Numerical Solution

In this section we discuss numerical method to solve the Eq. (13) and Eq. (14). We use MATLAB built-in function *bvp4c*. bvp4c is based on collocation technique. The basic functions used in *bvp4c* are bvp4c and bvpinit. To solve BVP in *bvp4c* we convert ODEs into a system of first orders ODE. Thus, first order ODE is:

$$u_1 = f,$$
$$u_2 = u_1',$$
$$u_3 = u_2',$$
$$u_4 = \theta,$$
$$u_5 = u_4'. \tag{19}$$

Then equation (13). and (14). are written to a system of first order ODEs that are as follow:

$$u_1' = u_2,$$
$$u_1'(0) = 0$$
$$u_2' = u_3,$$
$$u_2(0) = 1$$

$$\tag{20}$$

11

$$u_3' = \alpha u_5 u_3 + e^{\alpha u_4}\left(u_2^2 - u_1 u_3 + S\left(\frac{\eta}{2}u_3 + u_2\right) + \mathrm{M}u_2\right) + \gamma u_2, \, u_3(0) = \epsilon_1, \qquad (21)$$

$$u_4' = u_5,$$

$$u_5'(0) = \frac{-1}{1 + \mathrm{R} + \epsilon u_4(0)},$$

$$u_5' = \frac{1}{1 + \mathrm{R} + \epsilon u_4}\left(\mathrm{Pr}\left(r u_2 u_4 - u_5 + S\left(\frac{eta}{2}u_5 + m u_4\right)\right) - \epsilon u_5^2\right), \, u_5(0) = \epsilon_2,$$

12

Table 2.1: Contrast of $\theta(0)$ values when S = M = α = γ = 0, r = 1 with Parsad et al.[31] (for Newtonian case (n=1), $\epsilon = 0.0, 0.1$ and $\beta = 0$)

ϵ	Pr	Prasad et al.[31]	Present work
0	0.7	1.2470	1.2491
0	1.0	0.9986	0.9998
0	2.0	0.6575	0.6566
0	5.0	0.3922	0.3910
0.1	0.7	1.3714	1.3751
0.1	1.0	1.0758	1.0751
0.1	2.0	0.6894	0.6896
0.1	5.0	0.4032	0.4032

2.4   Validation of Method

Several wall temperature values $\theta(0)$, thermal conductivity parameter ϵ and Prandtl number Pr have been compared to those of the earlier steady-state problem of Prasad et al. [31] to assess the validity and correctness of the present numerical scheme. The results are displayed in table. It can be seen that, our results are very similar to those of Prasad et al. [31]

2.5 Results

Although there is a huge parameter domain to scout, we find that computations for bigger values of controlling parameters are especially difficult due to numerical convergence issues. As a result, we give data for a small set of physical factors selected to discuss the main patterns in this section. This section discusses the effects of the Darcy number γ, magnetic parameter M, radiation parameter R, viscosity parameter α, unsteadiness parameter S, Prandtl number Pr and variable thermal conductivity ϵ. The parameter values are M = 0.5, R = 1, Pr = 0.71, S = 0.5 and $\alpha = \epsilon = $ r = m = 0.4 as input to get the results. Figures (2.1)-(2.7) summarise the findings.

The variations of the magnetic parameter on velocity and temperature profiles are shown in Figures 2.1 (a) and 2.1 (b). The dimensionless temperature rises for boost up values of magnetic parameter M according to these figures. Inflation of the magnetic parameter causes velocity to decelerate, as shown in Figure 2.1 (a). The Lorentz is generated by increasing the Hartmann number.

Figures 2.2 (a) and 2.2 (b) show the impact of different R values on thermal and velocity profiles. It illustrates that when R increases, the thickness of the thermal boundary layer and the temperature distribution improve. Higher R values provide greater temperature to the fluid flow, resulting in an increase in temperature and thermal boundary layer thickness, whereas lower R values have the reverse effect (see Figure 2.2 (b)).

Figures 2.4 (a) and 2.4 (b) exhibit velocity and temperature curves for various values of the parameter γ, respectively. As shown in both figures, a bigger value of the γ parameter corresponds to a low velocity distribution and a high temperature distribution.

The graphical results in Figures 2.5 (a) and 2.5 (b) describe that as α increases, the velocity distribution decreases, while the sheet temperature $\theta(0)$ and dimensionless temperature rise.

The dimensionless velocity and temperature altering the unsteadiness parameter S are revealed in Figures 2.6 (a) and 2.6 (b). It's worth noting that the temperature has a maximum distribution when the unsteadiness parameter S is minimal, as a result

of the imposed thermal boundary condition. A similar pattern may be seen in the velocity profiles.

Figures 2.7 (a) and 2.7 (b) show the effect of various values of the ϵ on velocity and temperature. Figure 2.7 (a) convey that when the value of ϵ rises, the velocity also rises. Also, a bigger value of ϵ generates a significant shoot up in the temperature beside the sheet, as seen in Figure 2.7 (b).
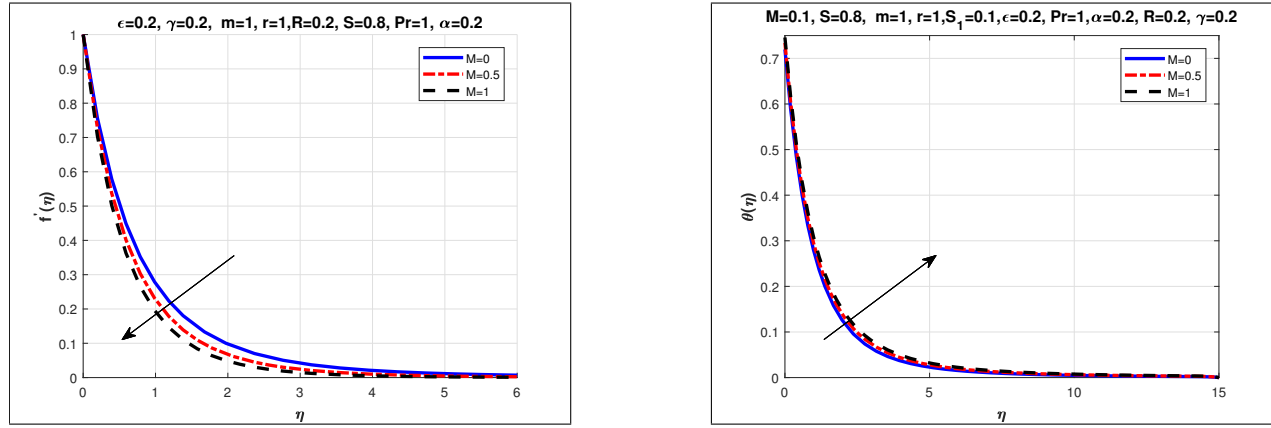
Figure 2.2: (a) Dimensionless Velocity for M. (b) Dimensionless Temperature for M.
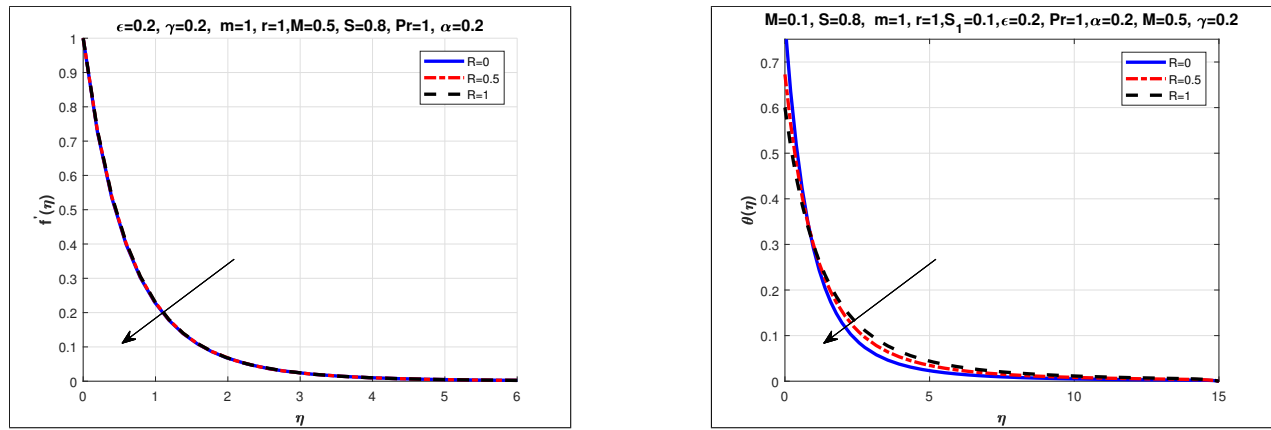
Figure 2.3: (a) Dimensionless Velocity for R. (b) Dimensionless Temperature for R.
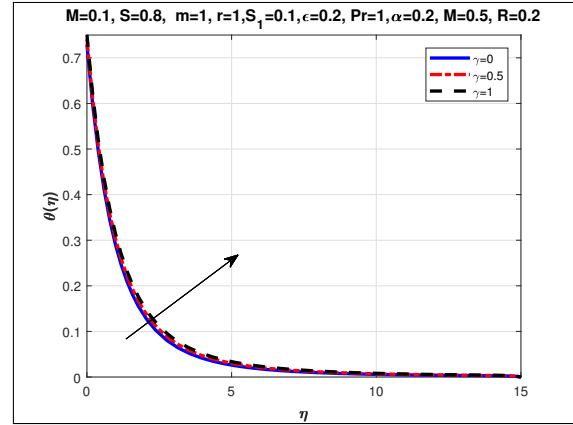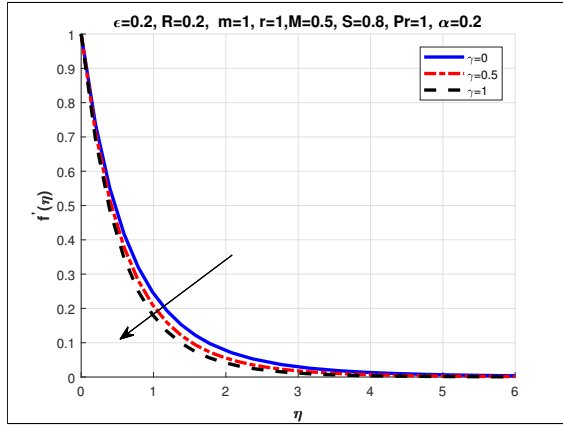
Figure 2.4: (*a*) Dimensionless Velocity for γ. (*b*) Dimensionless Temperature for γ.
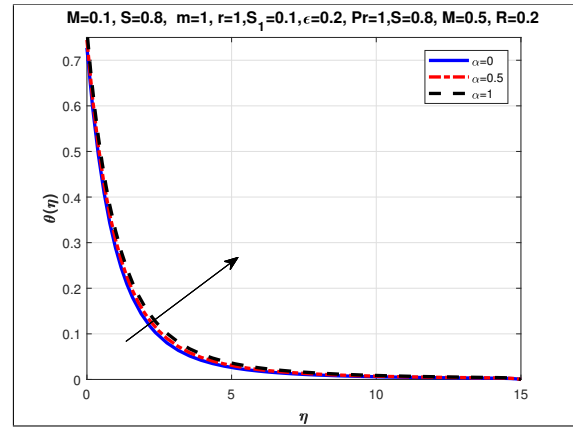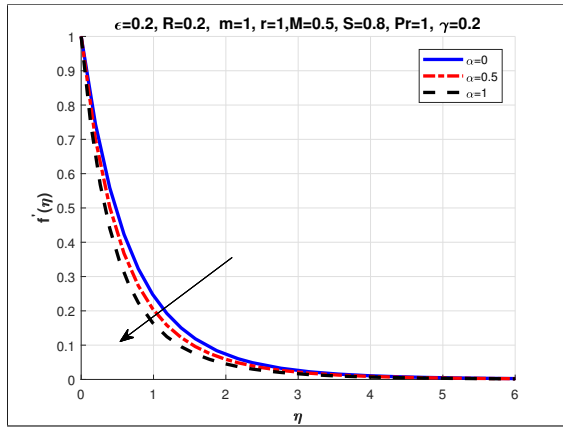
Figure 2.5: (*a*) Dimensionless Velocity for α. (*b*) Dimensionless Temperature for α.
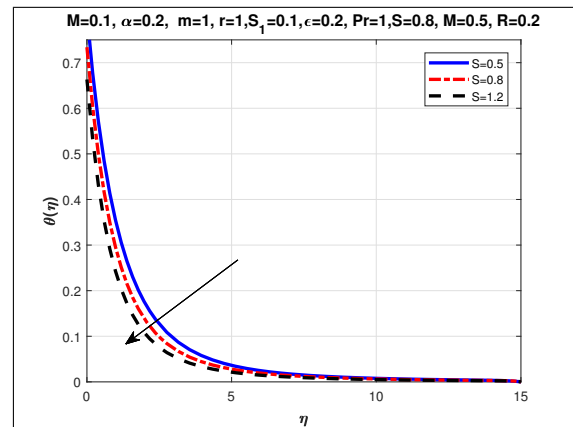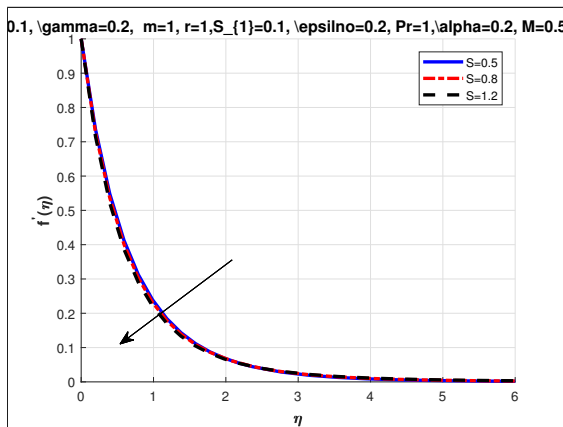
Figure 2.6: (*a*) Dimensionless Velocity for S. (*b*) Dimensionless Temperature for S.
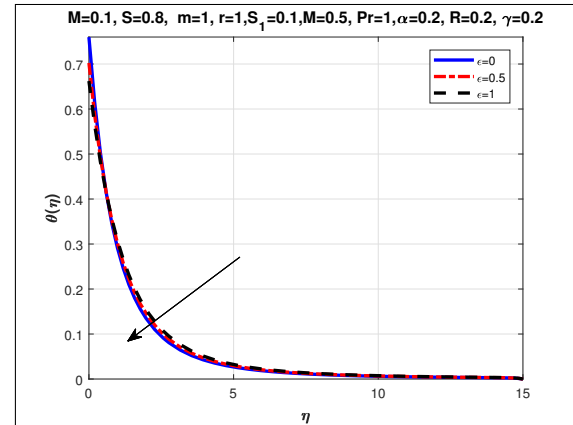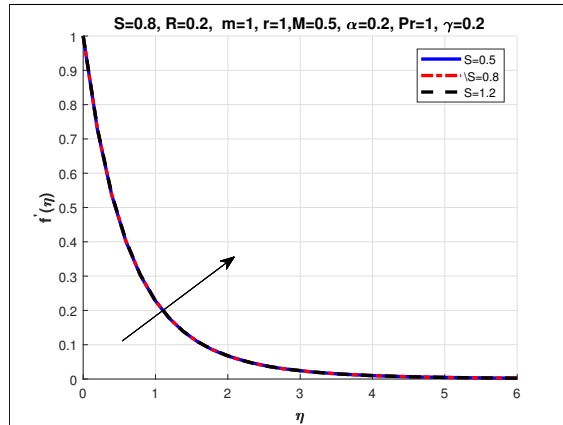
Figure 2.7: (a) Dimensionless Velocity for ϵ. (b) Dimensionless Temperature for ϵ.

Table 2 shows how changes in the ϵ, R, α, S, and M affect the Local Nusselt number and the Skin-friction coefficient. Table 2 shows that as the S, M, R, γ, and ϵ increase, so does skin-friction coefficient, whereas the Nusselt number rises as the S, ϵ, and R increase. Additionally, as the magnetic parameter, viscosity parameter, and Darcy number increase, the local Nusselt number drops.

Table 2.2: Fluctuations of skin friction and Nusselt number for several values of S, R, α, M, ϵ, γ, and R along with m=Pr=r=1.

M	R	γ	α	S	ϵ	$-f''(0)$	$\frac{1}{\theta(0)}$
0	0.2	0.2	0.2	0.8	0.2	1.25980	1.38944
0.5						1.42306	1.36269
1						1.56849	1.34093
0.5	0					1.41848	1.27138
	0.5					1.42861	1.48658
	1					1.43564	1.66778
	0.2	0				1.36686	1.37188
		0.5				1.50277	1.35021
		1				1.62566	1.33214
		0.2	0			1.51445	1.37507
			0.5			1.29007	1.34321
			1			1.08033	1.30834
			0.2	0.5		1.34063	1.23844
				0.8		1.42306	1.36269
				1.2		1.52572	1.50799
				0.5	0	1.42127	1.31627
				0.8	0.5	1.42538	1.42386
				1.2	1	1.42859	1.51041

Chapter 3

Maxwell Fluid Flow over an Unsteady Stretching Sheet with Variable Heat Flux

In this chapter we will discuss the flow of Maxwell fluid over an unsteady stretching sheet with variable heat flux. Section 3.1 discusses the flow model and mathematical formulation of the model, Section 3.2 discusses the numerical solution of the governing ODEs by using *bvp4c* in MATLAB. Then in Section 3.3 we discuss the validation of our proposed method, at last we will discuss the results with the help of graphs.

3.1 Flow Model

This section will introduce the appropriate description for all the governing equations of the laminar boundary layer fluid for an incompressible two dimensional viscous fluid flow and the heat devolve due to an unsteady stretching sheet. The governing physical properties are surface velocity, fluid velocity and thermal conductivity of fluid. Liu et al. [14] introduced in detail the Variable heat flux, which is also involved in this model.

$$q^*(x,t) = -\kappa_{eff}\frac{\partial T}{\partial y} = T_0\frac{dx^r}{(1-at)^{m+(\frac{1}{2})}},$$

(3.1)

where

$T_0=$ reference temperature,

19

$a=$ positive constant,

$d=$ constant,

$r=$ space index,

$m=$ time index,

And the applied transverse magnetic field B can be interpolated as follows [25]:

$$\text{B} = \frac{\text{B}_o}{(1 - at)^{\frac{1}{2}}} \tag{3.2}$$

where B_o is a constant.

This particular form for the B will allow the existence of the dimensionless magnetic field parameter commanding the velocity inside the boundary layer.

The supervised time-dependent boundary layer equations for mass,energy conservation and momentum are given by

$$u_x + v_y = 0, \tag{1}$$

$$u_t + uu_x + vu_y = \frac{1}{\rho_\infty}\left(\mu u_y\right)_y - \frac{\sigma \text{B}^2}{\rho_\infty}(u + \lambda_1 vu_y) - \frac{\mu u}{\rho_\infty k} - \lambda_1[u^2 u_{xx} + v^2 u_{yy} + 2uvu_{xy}], \tag{2}$$

$$T_t + uT_x + vT_y = \frac{1}{\rho_\infty C_p}(\kappa T_y)_y - \frac{1}{\rho_\infty C_p}(q_r)_y + \frac{\text{Q}}{\rho C_p}(T - T_\infty), \tag{3}$$

where u and v are the velocity components along the x and y directions, respectively. t, ρ_∞, μ, T, λ_1, κ, Q, C_p and σ is the time, fluid density, fluid viscosity,fluid temperature, relaxation time, permeability of the porous medium, heat source parameter, specific heat at constant pressure and the electrical conductivity respectively. q_r is the radiative heat flux as introduced by Parsad et al. [26] as follows:

$$q_r = -\frac{4\sigma^*}{3k^*}\frac{\partial T^4}{\partial y} \tag{4}$$

where σ^* is the Stefan Boltzmann constant and k^* is the Rosseland mean absorption coefficient. If the temperature differences within the flow are sufficiently small then by expending T^4 into Taylor series about T also neglecting the higher order terms. Then we get,

$$T^4 \approx 4T_\infty^3 T - 3T_\infty^4 \tag{3.3}$$

20

boundary condition corresponding to considered model is taken as,

$$u = U_w, v = 0, -\kappa_{eff}T_y = q(x,t) \quad \text{at} \quad y = 0, \tag{5}$$

$$u \to 0, T \to T_\infty \quad as \quad y \to \infty. \tag{6}$$

where

$$\kappa_{eff} = \kappa + \frac{16\sigma^* T_\infty^3}{3K^*}$$

T_∞ is the temperature of the fluid at the surrounding and U_w is the surface velocity which can be identified as:

$$\mathrm{U}_w = \frac{bx}{1 - at}. \tag{3.4}$$

The similarity variables are defined as:

$$\eta = \left(\frac{b}{\nu_\infty(1 - at)}\right)^{\frac{1}{2}} y \tag{7}$$

$$\psi = (\nu_\infty b)^{\frac{1}{2}} x f(\eta)$$

$$\theta(\eta) = \frac{T - T_\infty}{(\frac{q(x,t)}{\kappa_\infty})\sqrt{\frac{\nu_\infty}{b}}(1 - at)^{\frac{1}{2}}} \tag{8}$$

where the stream function is $\psi(x,t)$, ν_∞ is the kinematic viscosity at the surrounding, $\theta(\eta)$ and $f(\eta)$ are the dimensionless temperature and stream function respectively. The μ and κ depends on temperature as follows [32,33]:

$$\frac{\mu}{\mu_\infty} = e^{-\alpha\theta}, \frac{\kappa}{\kappa_\infty} = (1 + \epsilon\theta) \tag{9}$$

where μ_∞ is the viscosity at the surrounding, α is the dimensionless viscosity parameter,κ_∞ is the thermal conductivity away from the surface, and ϵ is the conductivity parameter. Now we will discuss two cases, case A (Constant Fluid Properties) and case B (Variable Fluid Properties).

3.1.1 Case A: Constant Fluid Properties

In Case A we keep α and ϵ as constant. Using Eq.(7) and Eq.(8) continuity equation (1) is satisfied.

$$u = \frac{\partial \psi}{\partial y}$$

21

Firstly we find values of terms.

$$u = \frac{bxf'}{1 - at},$$

$$v = -\frac{\partial \psi}{\partial x},$$

$$v = -\sqrt{\frac{\nu_\infty b}{1 - at}} f(\eta),$$

$$u_x + v_y = 0,$$

$$u_x = \frac{bf'}{1 - at},$$

$$v_y = -\frac{bf'}{1 - at},$$

now put all values in equation of continuity to satisfy it.

$$\frac{bf'}{1 - at} - \frac{bf'}{1 - at} = 0$$

$$0 = 0$$

equation of continuity is satisfied, now we will find momentum equation.

$$u_t + uu_x + vu_y = \frac{1}{\rho_\infty} \frac{\partial(\mu u_y)}{\partial y} - \frac{\sigma B^2 u}{\rho_\infty} - \frac{\mu u}{\rho_\infty \kappa} - \lambda_1 [u^2 u_{x^2} + v^2 u_{y^2} + 2uv u_{xy}],$$

22

firstly we find the values of all the terms and then insert in the equation.

$$u_t = \frac{abxf'}{(1-at)^2} + \frac{abx\eta f''}{2(1-at)^2},$$

$$u_x = \frac{bf'}{1-at},$$

$$uu_x = \frac{b^2xf'^2}{(1-at)^2},$$

$$u_y = \frac{bxf''}{1-at}\sqrt{\frac{b}{\nu_\infty}}\frac{1}{\sqrt{1-at}},$$

$$vu_y = -\frac{b^2ff''x}{1-at},$$

$$\frac{1}{\rho_\infty}\mu u_y = \frac{1}{\rho_\infty}\mu_\infty\frac{b^{\frac{3}{2}}xf''}{\sqrt{\nu_\infty}(1-at)^{\frac{3}{2}}},$$

$$\frac{1}{\rho_\infty}\frac{\partial}{\partial x}(\mu u_y) = \frac{\mu_\infty b^2xf'''}{\rho_\infty\nu_\infty(1-at)^2},$$

$$\frac{\mu u}{\rho_\infty\kappa} = \frac{\mu_\infty bxf'}{\rho_\infty\nu_\infty(1-at)\kappa},$$

Now we calculate

$$-\lambda_1[u^2u_{x^2} + v^2u_{y^2} + 2uvu_{xy}]$$

$$u^2u_{x^2} = 0,$$

$$v^2u_{y^2} = \frac{b^3xf^2f''}{(1-at)^3},$$

$$2uvu_{xy} = -\frac{2b^3xff'f''}{(1-at)^3},$$

Put values

$$-\lambda_1[u^2u_{x^2} + v^2u_{y^2} + 2uvu_{xy}] = -\lambda_1\left[\frac{b^3xf^2f''}{(1-at)^3} - \frac{2b^3xff'f''}{(1-at)^3}\right]$$

$$= -\frac{\lambda_1 b^3x}{(1-at)^3}(f^2f''' - 2ff'f''),$$

now

$$\frac{\sigma B^2}{\mu_\infty}(u + \lambda_1vu_y) = \frac{\sigma B^2 bx}{\mu_\infty(1-at)}(f' - Deff'')$$

23

Now put all values in momentum equation.

$$\frac{abxf'}{(1-at)^2} + \frac{abx\eta f''}{2(1-at)^2} + \frac{b^2xf'^2}{(1-at)^2} - \frac{b^2ff''x}{1-at} = \frac{\mu_\infty b^2xf'''}{\rho_\infty\nu_\infty(1-at)^2}$$

$$- \frac{\sigma B^2bx}{\mu_\infty(1-at)}(f' - Deff'') - \frac{\mu_\infty bxf'}{\rho_\infty\nu_\infty(1-at)\kappa}$$

$$- \frac{\lambda_1 b^3 x}{(1-at)^3}(f^2f''' - 2ff'f''),$$

multiply on both sides by $\frac{(1-at)^2}{b^2x}$,

$$\frac{a}{b}f' + f'^2 - ff'' + \frac{a}{2b}f''\eta = f''' - \frac{\sigma B_0^2}{\rho_\infty b}(f' - Deff'') - \frac{\mu_\infty}{\rho_\infty k_\infty b}(1-at)f' - \frac{\lambda_1 b}{(1-at)}\left(f^2f'' + 2ff'f''\right),$$

Now using

$$M = \frac{\sigma B^2}{b\rho_\infty}, \quad \gamma = \frac{\mu_\infty(1-at)}{\rho_\infty kb}, \quad De = \frac{\lambda_1(t)b}{(1-at)}, \quad S = \frac{a}{b}$$

$$Sf' + f'^2 + S\frac{\eta}{2}f'' - ff'' = e^{-\alpha\theta}(f''' - \theta'\alpha f'') - M(f' - Deff'') - e^{-\alpha\theta}\gamma f'$$
$$- De\left(f^2f'' + 2ff'f''\right),$$

$$e^{-\alpha\theta}(f''' - \theta'\alpha f'') - Mf' - e^{-\alpha\theta}\gamma f' - S\left(f' + \frac{\eta}{2}f''\right) - f'^2 + ff'' - De\left(f^2f'' + 2ff'f''\right) = 0,$$

$$f''' - M(f' - Deff'') - \gamma f' - S\left(f' + \frac{\eta}{2}f''\right) - f'^2 + ff'' - De\left(f^2f'' + 2ff'f''\right) = 0. \quad (10)$$

above equation is the momentum equation.

Now we solve for Energy equation.

$$T_t + uT_x + vT_y = \frac{1}{\rho_\infty C_p}\frac{\partial}{\partial y}(\kappa T_y) - \frac{1}{\rho_\infty C_p}(q_r)_y + \frac{Q}{\rho C_p}(T - T_\infty),$$

firstly we will find the values of terms that are included in the energy equation.

$$T_t = \frac{T_o dx^r}{\kappa_\infty}\sqrt{\frac{\nu_\infty}{b}}\frac{ma\theta}{(1-at)^{m+1}} + \frac{T_o dx^r a\eta}{2\kappa_\infty(1-at)^{m+1}}\sqrt{\frac{\nu_\infty}{b}}\theta',$$

$$uT_x = \frac{T_o dx^{2r}bf'}{\kappa_\infty(1-at)^{m+1}}\sqrt{\frac{\nu_\infty}{b}}\theta,$$

24

$$vT_y = -\frac{T_o dx^r f}{\kappa_\infty (1-at)^{m+1}} \sqrt{\nu_\infty b} \theta',$$

$$\frac{1}{\rho_\infty C_p} \frac{\partial}{\partial y}(\kappa T_y) = \frac{1}{\rho_\infty C_p} \frac{T_o dx^r (1+\theta)}{(1-at)^{m+1}} \sqrt{\frac{b}{\nu_\infty}},$$

$$\frac{1}{\rho_\infty C_p}(q_r)_y = -\frac{16T_\infty^3}{\rho_\infty C_p 3K^*} \frac{\sigma^* T_o dx^r}{\kappa_\infty (1-at)^{m+1}} \sqrt{\frac{b}{\nu_\infty}} \theta'',$$

$$\frac{Q}{\rho C_p}(T - T_\infty) = \frac{Q_o T_o dx^r}{\rho C_p \kappa_\infty (1-at)^{m+\frac{1}{2}}} \sqrt{\frac{\nu_\infty}{b}} \theta,$$

putting all values in the energy equation we get,

$$\frac{T_o dx^r}{\kappa_\infty} \sqrt{\frac{\nu_\infty}{b}} \frac{ma\theta}{(1-at)^{m+1}} + \frac{T_o dx^r a\eta}{2\kappa_\infty (1-at)^{m+1}} \sqrt{\frac{\nu_\infty}{b}} \theta'$$

$$+ \frac{T_o dx^{2r} b f'}{\kappa_\infty (1-at)^{m+1}} \sqrt{\frac{\nu_\infty}{b}} \theta - \frac{T_o dx^r f}{\kappa_\infty (1-at)^{m+1}} \sqrt{\nu_\infty b} \theta' =$$

$$\frac{1}{\rho_\infty C_p} \frac{T_o dx^r (1+\theta)}{(1-at)^{m+1}} \sqrt{\frac{b}{\nu_\infty}} + \frac{16T_\infty^3}{\rho_\infty C_p 3K^*} \frac{\sigma^* T_o dx^r}{\kappa_\infty (1-at)^{m+1}} \sqrt{\frac{b}{\nu_\infty}}$$

$$+ \frac{Q_o T_o dx^r}{\rho C_p \kappa_\infty (1-at)^{m+\frac{1}{2}}} \sqrt{\frac{\nu_\infty}{b}} \theta,$$

multiply the above equation on both sides by $\frac{(1-at)^{m+1}\kappa_\infty}{\sqrt{\nu_\infty b}T_o dx^r}$,

we get,

$$\frac{a}{b}m\theta + \frac{a}{b}\eta\theta' + f'r\theta - f\theta' = \frac{(1+\theta)\kappa_\infty}{\rho_\infty C_p \nu_\infty}\theta'' + \frac{1}{\rho_\infty C_p \nu_\infty}\left(\frac{16T_\infty^3\sigma^*}{3K^*\kappa_\infty}\right) + \frac{Q_o(1-at)^{\frac{1}{2}}}{\rho C_p b},$$

now using the non-dimentional parameters in above equation;

$$S = \frac{a}{b}, R = \frac{16\sigma^* T_\infty^3}{3\kappa_\infty K^*}, Pr = \frac{\mu_\infty C_p}{\kappa_\infty}, \rho_\infty = \frac{\mu_\infty}{\nu_\infty}, S_1 = \frac{Q_o x}{\rho C_p U_w}$$

$$\frac{R}{Pr}\theta'' + \frac{(1+\theta)}{Pr}\theta'' + f\theta' - rf'\theta - S\left(\frac{\eta}{2}\theta + m\theta\right) + S_1\theta = 0$$

$$\frac{1}{Pr}\left(1 + R + \theta\right)\theta'' + f\theta' - rf'\theta - S\left(\frac{\eta}{2}\theta' + m\theta\right) + S_1\theta = 0 \qquad (11)$$

Above equation is the Energy equation. The corresponding boundary conditions are;

$$f(0) = 0 f'(0) = 1, \theta'(0) = -\frac{1}{1+R} \qquad (12)$$

$$f' \to 0, \qquad \theta \to 0 \;\; as \;\; \eta \to \infty \qquad (13)$$

where R is the radiation parameter, $M = \frac{\sigma B^2}{b\rho_\infty}$ is the magnetic field, $R = \frac{16\sigma^* T_\infty^3}{3\kappa_\infty k*}$ is the radiation parameter, $Pr = \frac{\mu_\infty c_p}{\kappa_\infty}$ is the Prandtl number, $\gamma = \frac{\mu_\infty (1-at)}{\rho_\infty kb}$ is the local Darcy number, $S = \frac{a}{b}$ is the unsteadiness parameter, $S_1 = \frac{Q_o x}{\rho C p U_w}$ is the heat generation/absorption parameter, $De = \frac{\lambda_1(t)b}{(1-at)}$ is the Deborah number. $\lambda_1 = \lambda_o(1-at)$ can be taken for similarity solution λ_1, then $De = b\lambda_o$, where λ_o is a constant.

3.1.2   Case B: Variable Fluid Properties

Case B is the Variable Fluid properties. Using Eq.(7) and Eq.(8) continuity Eq.(1) is satisfied.

$$u = \frac{\partial \psi}{\partial y},$$

firstly we find values of terms.

$$u = \frac{bx f'}{1 - at},$$

$$v = -\frac{\partial \psi}{\partial x},$$

$$v = -\sqrt{\frac{\nu_\infty b}{1 - at}} f(\eta),$$

$$u_x + v_y = 0,$$

$$u_x = \frac{b f'}{1 - at},$$

$$v_y = -\frac{b f'}{1 - at},$$

now put all values in equation of continuity to satisfy it.

$$\frac{b f'}{1 - at} - \frac{b f'}{1 - at} = 0,$$

$$0 = 0$$

equation of continuity is satisfied, now we will find momentum equation.

$$u_t + u u_x + v u_y = \frac{1}{\rho_\infty} \frac{\partial(\mu u_y)}{\partial y} - \frac{\sigma B^2 u}{\rho_\infty} - \frac{\mu u}{\rho_\infty \kappa} - \lambda_1 [u^2 u_{x^2} + v^2 u_{y^2} + 2uv u_{xy}],$$

26

firstly we find the values of all the terms and then insert in the equation.

$$u_t = \frac{abx f'}{(1-at)^2} + \frac{abx\eta f''}{2(1-at)^2},$$

$$u_x = \frac{bf'}{1-at},$$

$$uu_x = \frac{b^2 x f'^2}{(1-at)^2},$$

$$u_y = \frac{bx f''}{1-at}\sqrt{\frac{b}{\nu_\infty}}\frac{1}{\sqrt{1-at}},$$

$$vu_y = -\frac{b^2 f f'' x}{1-at},$$

$$5\frac{1}{\rho_\infty}\mu u_y = \frac{1}{\rho_\infty}\mu_\infty e^{-\alpha\theta}\frac{b^{\frac{3}{2}} x f''}{\sqrt{\nu_\infty}(1-at)^{\frac{3}{2}}},$$

$$\frac{1}{\rho_\infty}\frac{\partial}{\partial x}(\mu u_y) = -\frac{\mu_\infty b^2 x\alpha e^{-\alpha\theta}\theta' f''}{\rho_\infty\nu_\infty(1-at)^2} + \frac{\mu_\infty b^2 x e^{-\alpha\theta} f'''}{\rho_\infty\nu_\infty(1-at)^2},$$

$$\frac{\sigma B^2 u}{\rho_\infty} = \frac{\sigma B^2 bx}{\rho_\infty(1-at)}(f' - Def f''),$$

$$\frac{\mu u}{\rho_\infty\kappa} = \frac{\mu_\infty bx e^{-\alpha\theta} f'}{\rho_\infty\nu_\infty(1-at)\kappa},$$

Now we calculate

$$-\lambda_1[u^2 u_{x^2} + v^2 u_{y^2} + 2uv u_{xy}],$$

$$u^2 u_{x^2} = 0,$$

$$v^2 u_{y^2} = \frac{b^3 x f^2 f''}{(1-at)^3},$$

$$2uv u_{xy} = -\frac{2b^3 x f f' f''}{(1-at)^3},$$

Put values

$$-\lambda_1[u^2 u_{x^2} + v^2 u_{y^2} + 2uv u_{xy}] = -\lambda_1\left[\frac{b^3 x f^2 f''}{(1-at)^3} - \frac{2b^3 x f f' f''}{(1-at)^3}\right]$$

$$= -\frac{\lambda_1 b^3 x}{(1-at)^3}(f^2 f''' - 2f f' f''),$$

27

Now put all values in momentum equation.

$$\frac{abx f'}{(1-at)^2} + \frac{abx\eta f''}{2(1-at)^2} + \frac{b^2 x f'^2}{(1-at)^2} - \frac{b^2 f f'' x}{1-at} = -\frac{\mu_\infty b^2 x \alpha e^{-\alpha\theta} \theta' f''}{\rho_\infty \nu_\infty (1-at)^2} + \frac{\mu_\infty b^2 x e^{-\alpha\theta} f'''}{\rho_\infty \nu_\infty (1-at)^2}$$
$$-\frac{\sigma B^2 b x}{\rho_\infty (1-at)} (f' - De f f'') - \frac{\mu_\infty b x e^{-\alpha\theta} f'}{\rho_\infty \nu_\infty (1-at)\kappa}$$
$$-\frac{\lambda_1 b^3 x}{(1-at)^3} (f^2 f''' - 2 f f' f''),$$

$$\frac{abx f'}{(1-at)^2} + \frac{abx\eta f''}{2(1-at)^2} + \frac{b^2 x f'^2}{(1-at)^2} - \frac{b^2 f f'' x}{1-at} = -\frac{\mu_\infty b^2 x}{\rho_\infty \nu_\infty (1-at)^2}\left(-\alpha e^{-\alpha\theta} \theta' f'' + e^{-\alpha\theta} f'''\right)$$
$$-\frac{\sigma B_0^2 b x}{\rho_\infty (1-at)^2} (f' - De f f'') - \frac{\mu_\infty b x e^{-\alpha\theta} f'}{\rho_\infty \nu_\infty (1-at)\kappa}$$
$$-\frac{\lambda_1 b^3 x}{(1-at)^3} (f^2 f''' - 2 f f' f''),$$

multiply on both sides by $\frac{(1-at)^2}{b^2 x}$

$$\frac{a}{b} f' + f'^2 - f f'' + \frac{a}{2b} f'' \eta = \left(-e^{-\alpha\theta} f'' + e^{-\alpha\theta} f'''\right) - \frac{\sigma B_0^2}{\rho_\infty b}(f' - De f f'') - \frac{\mu_\infty}{\rho_\infty k_\infty b}(1-at) f' e^{-\alpha\theta}$$
$$-\frac{\lambda_1 b}{(1-at)}\left(f^2 f'' + 2 f f' f''\right),$$

Now using

$$M = \frac{\sigma B^2}{b\rho_\infty}, \quad \gamma = \frac{\mu_\infty (1-at)}{\rho_\infty kb}, \quad De = \frac{\lambda_1(t) b}{(1-at)}, \quad S = \frac{a}{b}$$

$$S f' + f'^2 + S\frac{\eta}{2} f'' - f f'' = e^{-\alpha\theta}\left(f''' - \theta'\alpha f''\right) - M(f' - De f f'') - e^{-\alpha\theta}\gamma f'$$
$$-De\left(f^2 f'' + 2 f f' f''\right),$$
$$e^{-\alpha\theta}\left(f''' - \theta'\alpha f''\right) - M(f' - De f f'') - e^{-\alpha\theta}\gamma f' -$$
$$S\left(f' + \frac{\eta}{2} f''\right) - f'^2 + f f'' - De\left(f^2 f''| + 2 f f' f''\right) = 0,$$

$$e^{-\alpha\theta}\left(f''' - \theta'\alpha f''\right) - M(f' - De f f'') - e^{-\alpha\theta}\gamma f' - S\left(f' + \frac{\eta}{2} f''\right) - f'^2 + f f'' - De\left(f^2 f'' + 2 f f' f''\right) = 0.$$
$$(14)$$

28

above equation is the momentum equation.

Now we solve for Energy equation.

$$T_t + uT_x + vT_y = \frac{1}{\rho_\infty C_p}\frac{\partial}{\partial y}(\kappa T_y) - \frac{1}{\rho_\infty C_p}(q_r)_y + \frac{Q}{\rho C_p}(T - T_\infty),$$

firstly we will find the values of terms that are included in the energy equation.

$$T_t = \frac{T_o dx^r}{\kappa_\infty}\sqrt{\frac{\nu_\infty}{b}}\frac{ma\theta}{(1 - at)^{m+1}} + \frac{T_o dx^r a\eta}{2\kappa_\infty (1 - at)^{m+1}}\sqrt{\frac{\nu_\infty}{b}}\theta',$$

$$uT_x = \frac{T_o dx^{2r} b f'}{\kappa_\infty (1 - at)^{m+1}}\sqrt{\frac{\nu_\infty}{b}}\theta,$$

$$vT_y = -\frac{T_o dx^r f}{\kappa_\infty (1 - at)^{m+1}}\sqrt{\nu_\infty b}\theta',$$

$$\frac{1}{\rho_\infty C_p}\frac{\partial}{\partial y}(\kappa T_y) = \frac{1}{\rho_\infty C_p}\frac{T_o dx^r (1 + \epsilon\theta)}{(1 - at)^{m+1}}\sqrt{\frac{b}{\nu_\infty}} + \frac{T_o dx^r \epsilon}{\rho_\infty C_p (1 - at)^{m+1}}\sqrt{\frac{b}{\nu_\infty}}\theta'^2,$$

$$\frac{1}{\rho_\infty C_p}(q_r)_y = -\frac{16T_\infty^3}{\rho_\infty C_p 3K^*}\frac{\sigma^* T_o dx^r}{\kappa_\infty (1 - at)^{m+1}}\sqrt{\frac{b}{\nu_\infty}}\theta'',$$

$$\frac{Q}{\rho C_p}(T - T_\infty) = \frac{Q_o T_o dx^r}{\rho C p \kappa_\infty (1 - at)^{m+\frac{1}{2}}}\sqrt{\frac{\nu_\infty}{b}}\theta,$$

putting all values in the energy equation we get,

$$\frac{T_o dx^r}{\kappa_\infty}\sqrt{\frac{\nu_\infty}{b}}\frac{ma\theta}{(1 - at)^{m+1}} + \frac{T_o dx^r a\eta}{2\kappa_\infty (1 - at)^{m+1}}\sqrt{\frac{\nu_\infty}{b}}\theta'$$

$$+ \frac{T_o dx^{2r} b f'}{\kappa_\infty (1 - at)^{m+1}}\sqrt{\frac{\nu_\infty}{b}}\theta - \frac{T_o dx^r f}{\kappa_\infty (1 - at)^{m+1}}\sqrt{\nu_\infty b}\theta' =$$

$$\frac{1}{\rho_\infty C_p}\frac{T_o dx^r (1 + \epsilon\theta)}{(1 - at)^{m+1}}\sqrt{\frac{b}{\nu_\infty}} + \frac{T_o dx^r \epsilon}{\rho_\infty C_p (1 - at)^{m+1}}\sqrt{\frac{b}{\nu_\infty}}\theta'^2$$

$$+ \frac{16T_\infty^3}{\rho_\infty C_p 3K^*}\frac{\sigma^* T_o dx^r}{\kappa_\infty (1 - at)^{m+1}}\sqrt{\frac{b}{\nu_\infty}} + \frac{Q_o T_o dx^r}{\rho C_p \kappa_\infty (1 - at)^{m+\frac{1}{2}}}\sqrt{\frac{\nu_\infty}{b}}\theta,$$

multiply the above equation on both sides by $\frac{(1-at)^{m+1}\kappa_\infty}{\sqrt{\nu_\infty b}T_o dx^r}$, we get,

$$\frac{a}{b}m\theta + \frac{a}{b}\eta\theta' + f'r\theta - f\theta' = \frac{(1 + \epsilon\theta)\kappa_\infty}{\rho_\infty C_p \nu_\infty}\theta'' + \frac{\epsilon\theta'^2}{\rho_\infty C_p \nu_\infty} + \frac{1}{\rho_\infty C_p \nu_\infty}\left(\frac{16T_\infty^3\sigma^*}{3K^*\kappa_\infty}\right) + \frac{Q_o(1 - at)^{\frac{1}{2}}}{\rho C_p b},$$

now using the non-dimentional parameters in above equation:

$$\mathrm{S} = \frac{a}{b}, \quad \mathrm{R} = \frac{16\sigma^* T_\infty^3}{3\kappa_\infty K^*}, \quad \mathrm{Pr} = \frac{\mu_\infty Cp}{\kappa_\infty}, \quad \rho_\infty = \frac{\mu_\infty}{\nu_\infty}, \quad \mathrm{S}_1 = \frac{Q_o x}{\rho C_p U_w}.$$

$$\frac{\mathrm{R}}{Pr}\theta'' + \frac{\epsilon}{Pr}\theta'^2 + \frac{(1+\epsilon\theta)}{Pr}\theta'' + f\theta' - rf'\theta - \mathrm{S}\left(\frac{\eta}{2}\theta + m\theta\right) + \mathrm{S}_1\theta = 0,$$

$$\frac{1}{Pr}\left[(1+\mathrm{R}+\epsilon\theta)\theta'' + \epsilon\theta'^2\right] + f\theta' - rf'\theta - \mathrm{S}\left(\frac{\eta}{2}\theta' + m\theta\right) + \mathrm{S}_1\theta = 0. \tag{15}$$

Above equation is the energy equation. The corresponding boundary conditions are;

$$f(0) = 0, f'(0) = 1, \theta'(0) = -\frac{1}{1+\epsilon\theta+\mathrm{R}}, \tag{16}$$

$$f' \to 0, \qquad \theta \to 0 \;\; as \;\; \eta \to \infty. \tag{17}$$

where ϵ is the conductivity parameter. It can be noted that the velocity and temperature fields are coupled to each other, that can be seen in Eq. (12) and Eq. (13). Crane [26] solved the velocity field systematically for steady problem S = 0, R = 0, M = 0, $\gamma = 0$ i.e when the thermal radiation, porous parameter and magnetic field are not present and $\alpha = 0$ i.e. viscosity is not a function of temperature, with $f = 1 - e^{-\eta}$.

3.2 Physical Parameters

The dimensionless physical parameters the skin friction coefficient and local Nusselt number are defined as:

3.2.1 Skin-Friction Coefficient:

The skin-Friction coefficient is written as;
Constant Fluid Properties

$$Cf_x = -2Re_x^{-\frac{1}{2}}f''(0) \tag{14}$$

Variable fluid Properties

$$Cf_x = -e^{-\alpha\theta}Re_x^{-\frac{1}{2}}f''(0) \tag{15}$$

30

3.2.2 Local Nusselt Number:

The local Nusselt number is written as:

$$Nu_x = \frac{Re_x^{\frac{1}{2}}}{\theta(0)}$$

where $Re_x = \frac{U_w x}{\nu_\infty}$ is the local Reynolds number.

3.3 Numerical Solution

We will solve for both cases for Constant, and variable fluid properties.

3.3.1 Case A: Constant Fluid Properties

The boundary value problem (Bvp) stated by equation (10) and (11) with boundary conditions (12) and (13) is solved using MATLAB package *bvp4c*.

$$y_1 = f \Rightarrow y_1' \quad = f' = y_2$$

$$y_2 = f' \Rightarrow y_2' \quad = f'' = y_3$$

$$y_3 = f'' \Rightarrow y_3' \quad = f''' = \frac{1}{1 - Dey_1^2}\left(M(y_2 - Dey_1y_3) + \gamma y_2 + S(y_2 + y_3\frac{\eta}{2}) + y_2^2 - y_1y_3 - 2Dey_1y_2\right)$$

$$y_4 = \theta \Rightarrow y_4' \quad = \theta' = y_5$$

$$y_5 = \theta \Rightarrow y_5' \quad = \theta'' = \frac{1}{(1 + R)}Pr(rf'\theta - f\theta' + S(\frac{\eta}{2}\theta' + m\theta) - \epsilon(\theta')^2 - S +_1 \theta)$$

31

3.3.2 Case B: Variable Fluid Properties

The boundary value problem (bvp) stated by equation (14) and (15) with boundary conditions (16) and (17) is solved using MATLAB package *bvp4c*.

$$y_1 = f \Rightarrow y_1' = f' = y_2, y_2 = f' \Rightarrow y_2' = f'' = y_3$$

$$y_3 = f'' \Rightarrow y_3' = f''' = \frac{1}{e^{-\alpha y_4} - De y_1^2}$$

$$\left(e^{-\alpha y_4} \alpha y_5 y_3 + M(y_2 - De y_1 y_3) + \gamma e^{-\alpha y_4} y_2 + S(y_2 + y_3 \frac{\eta}{2}) + y_2^2 - y_1 y_3 - 2De y_1 y_2 y_3 \right)$$

$$y_4 = \theta \Rightarrow y_4' = \theta' = y_5, y_5 = \theta \Rightarrow y_5' = \theta'' = \frac{1}{(1 + R + \epsilon\theta)} Pr(rf'\theta - f\theta'$$

$$+ S(\frac{\eta}{2}\theta' + m\theta) - \epsilon(\theta')^2 - S +_1 \theta)$$

3.4 Validation of Method

Comparison of constant and variable fluid properties with variable heat flux over a sheet for Maxwell fluid is done by using technique of *bvp4c* in MATLAB. To know the accuracy and reliability of the current numerical results, various values of Deborah number De have been compared to those of former problems of Abel et al. [34] and Megahed et al. [22]. The results of contrast/comparison are given in table 1.

3.5 Results and Discussion

In this section, we present the results of some physical parameteres that are selected to discuss the major trends. Impact of viscosity parameter, Deborah number, thermal conductivity, Darcy number, magnetic parameter, radiation parameter, unsteadiness parameter, heat generation/absorption parameter, Prandtl number is discussed in this section. The values of the parameters are $\alpha = R = \gamma = \epsilon = 0.2$, $S_1 = De = 0.1$, $M = 0.5$, $S = 0.8$, $Pr = r = m = 1$ as input to get results for complete production. Figure 3.1 (a) shows the effect of M which is the magnetic parameter on the flow velocity $f'(\eta)$. The flow velocity decreases slightly as M increases in Figure 3.1 (a) due to the applied transverse magnetic field which yields a drag force in the form of the

Lorentz force, reducing the magnitude of the velocity. Meanwhile, as seen in Figure 3.1 (b), as the magnetic field M is increased, the temperature of the flow gradually increases.

Figures 3.2 (a) and 3.2 (b) under the effect of the parameter ϵ estimate both the dimensionless velocity and temperature of an unsteady flow of non-Newtonian fluid with varying ϵ. The velocity $f'(\eta)$ values of ϵ are negligible, as seen in Figure 3.2 (a). Also, a huge conductivity parameter causes a significant fall in the temperature beside the sheet, as shown in Figure 3.2 (b).

The impact of increasing the parameter α on dimensionless velocity can be seen in Figure 3.3 (a), which leads to a drop in dimensionless velocity $f'(\eta)$. Similarly, raising the value of the same parameter raises the dimensionless temperature, as seen in Figure 3b.

In figures 3.4 (a) and 3.4 (b) shows the effect of Darcy number γ on $f'(\eta)$ and $\theta(\eta)$ respectively. When γ increases the velocity profile decreases. It is discovered that when Darcy number increases, the permeability of the porous medium decreases, resulting in a marked reduction in fluid activity. While the temperature profile increases with the increase in γ. The reason for this is because when the Darcy number rises, the fluid permeability of porous substances rises, and colder fluid's interaction with heated walls decreases. As a result, the temperature difference between the porous substance and the wall between them increases, and the dimensionless temperature rises with it.

Figures 3.5 (a) and 3.5 (b) depict the evolution of the velocity and temperature fields on the boundary layer region as a function of the R values for the thermal radiation parameter. As can be seen in Figure 3.5 (a), the magnitude of the velocity increases slowly as R rises. In addition, the temperature inside the thermal boundary layer, where the change in the R takes place, firstly falls and then rises.

The effect of De on the dimensionless velocity can be seen in figure 3.6 (a). It can be seen that increase in De results the lower value of the dimensionless velocity at any givenpoint above the sheet. Figure 3.6 (b) illustrates that at any point the dimensionless temperature $\theta(\eta)$ rises with the rising Deborah number. So, by choosing a coolant

33

which have a small De, can improve the cooling of the heated sheet.

The focus is now on the curves that show how the unsteadiness parameter S affects the dimensionless velocity and the temperature . These curves are shown in Figures 3.7 (a) and 3.7 (b), respectively. It's worth noting that as the unsteadiness parameter is increased, the velocity profile drops. While, with an increase in S, the temperature drops. This demonstrates the essential fact that the rate of cooling is much faster for higher values of the S, but smaller values of the S may take longer to cool.

Figure 8a and 8b shows the effect of heat generation and absorption parameter S_1. $f'\eta$ decreases as S_1 decreases so does momentum boundary layer thickness. While, the $\theta(\eta)$ increases with the increase in S_1.   Table 2 is presented to illustrate the behaviour
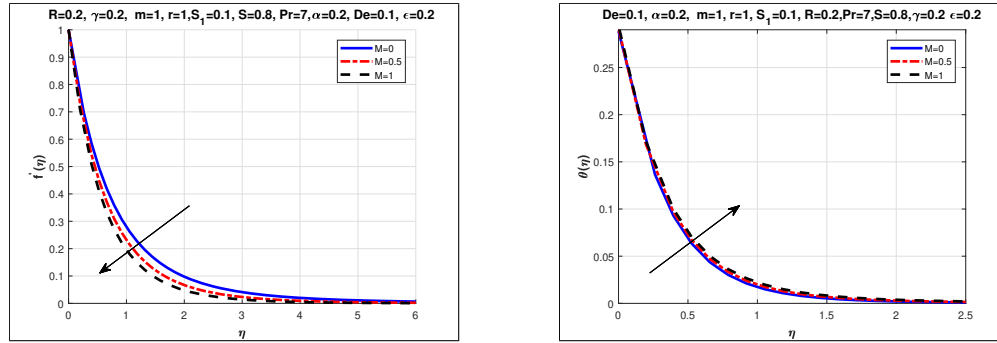

Figure 3.1: (a) Dimensionless Velocity for M. (b) Dimensionless Temperature for M.
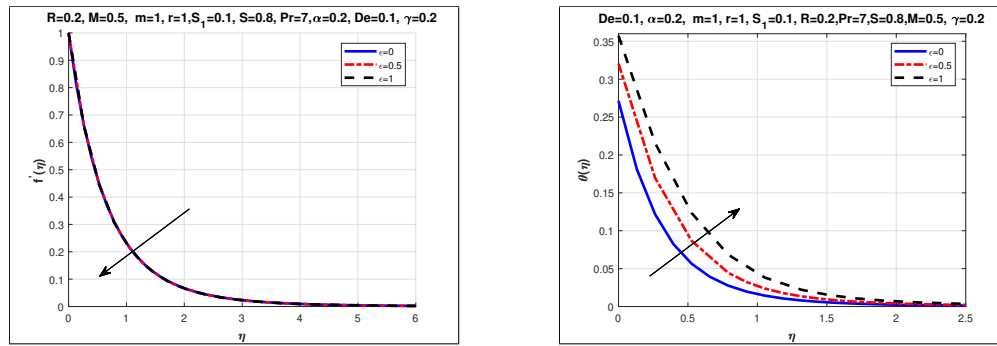

Figure 3.2: (a) Dimensionless Velocity for ϵ. (b)Dimensionless Temperature for ϵ.

of the Skin-friction Coefficient and the Local Nusselt Number with variations in viscosity parameter, Deborah Number, thermal conductivity, Darcy number, magnetic

Figure 3.3: (a) Dimensionless Velocity for α. (b) Dimensionless Temperature for α.

Figure 3.4: (a) Dimensionless Velocity for γ. (b) Dimensionless Temperature for γ.
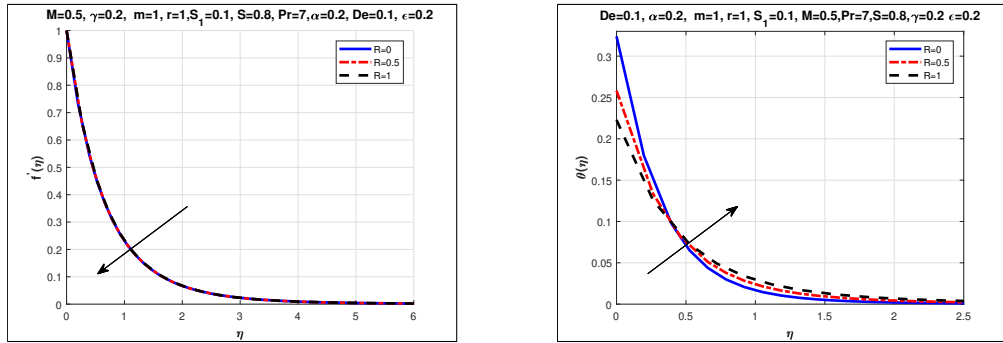
Figure 3.5: (a) Dimensionless Velocity for R. (b) Dimensionless Temperature for R.

parameter, radiation parameter,unsteadiness parameter, heat generation/absorption parameter for both Case A and Case B, and then a comparison is done between them by compairing the trend of local skin-friction coefficient and the local Nusselt number. For Case A the skin friction rises with the greater values of M, S, γ, and De. While α, R, ϵ and S_1 remains constant.The local Nusselt number falls with the rising values of
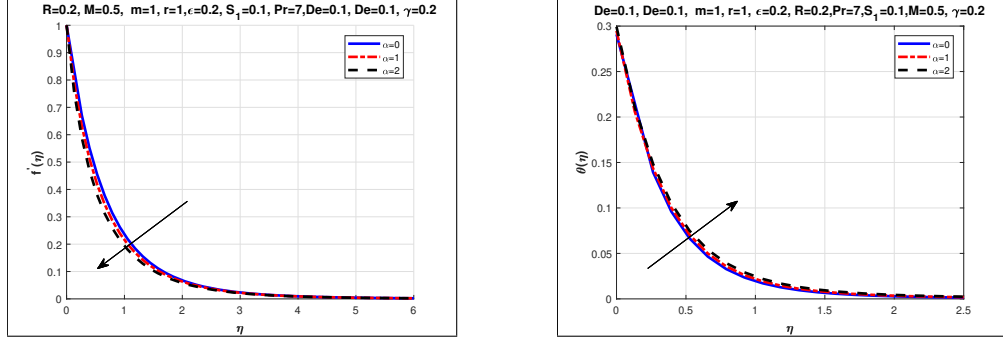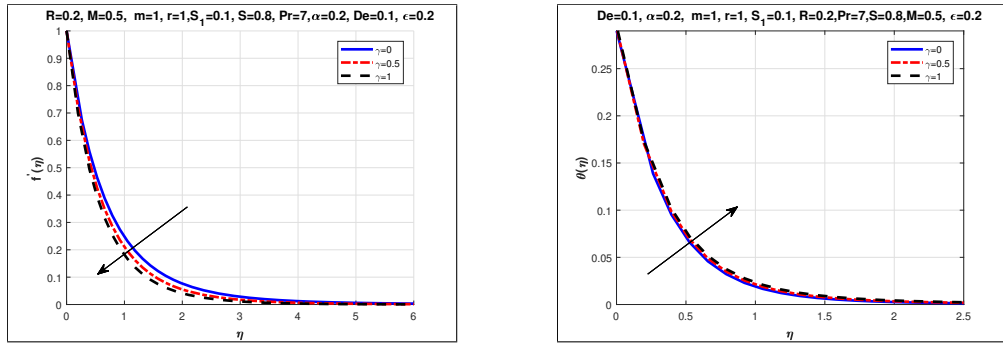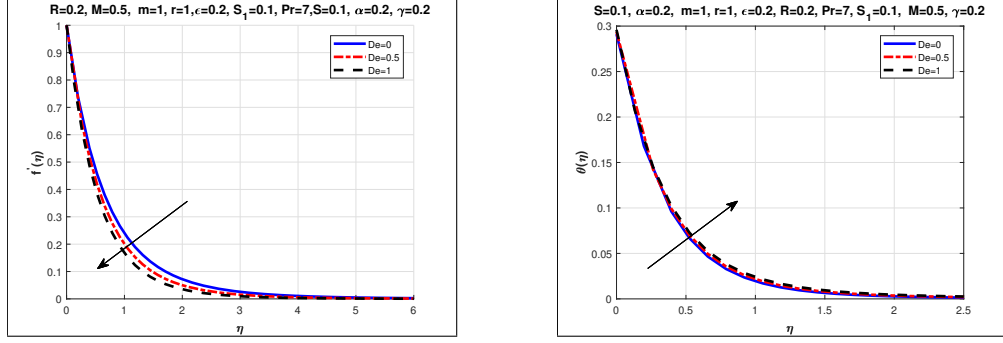
Figure 3.6: (*a*) Dimensionless Velocity for De. (*b*) Dimensionless Temperature for De.
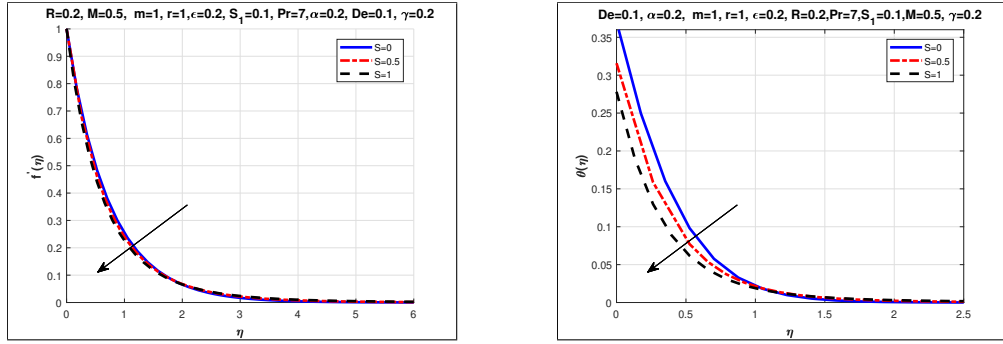
Figure 3.7: (*a*) Dimensionless Velocity for S. (*b*) Dimensionless Temperature distribution for S.
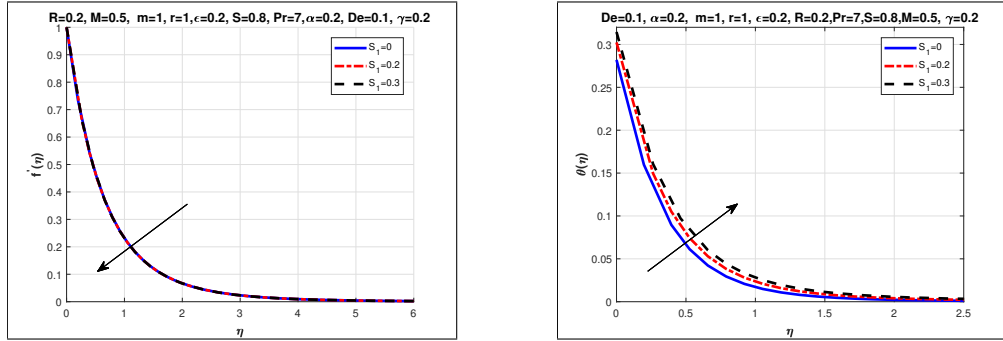
Figure 3.8: (*a*) Dimensionless Velocity for S_1. (*b*) Dimensionless Temperature for S_1.

M, γ, S_1 and De. And it remains constant with the higher values of α.

Now for Case B the skin-friction rises with the rising values of M, γ, α, S, ϵ and De. The local Nusselt number boost up with the rising values of R and ϵ. while it falls with the rising values of M, γ, α, S, S_1 and De.

Table 3.1: Contrast of skin friction coefficient for different value of De.

D_e	Abel et al.[34]	Megahed et al.[22]	Present Work
0	0.999962	0.999978	0.999999
0.2	1.051948	1.051945	1.051844
0.4	1.101850	1.101848	1.101883
0.6	1.150163	1.150160	1.150161
0.8	1.196692	1.196690	1.196666
1.2	1.285257	1.285253	1.285255
1.6	1.368641	1.368641	1.368642
2	1.447617	1.447616	1.447615

Table 3.2: Variation of skin friction and local Nusselt number for both Constant and Variable fluid properties, when $r = m = 1, \mathrm{Pr} = 7$.

M	R	γ	α	S	ϵ	S_1	De	CFP		VFP	
								$-f''(0)$	$\frac{1}{\theta(0)}$	$-e^{-\alpha\theta}f''(0)$	$\frac{1}{\theta(0)}$
0	0.2	0.2	0.2	0.8	0.2	0.1	0.1	1.3566	3.8210	1.3345	3.5381
0.5								1.5395	3.7820	1.5098	3.5026
1								1.6952	3.7478	1.6663	3.4685
0.5	0.1							1.5359	3.6339	1.5090	3.3305
	0.5							1.5359	4.1873	1.5118	3.9576
	1							1.5359	4.7677	1.5139	4.5917
	0.2	0						1.4691	3.7963	1.4464	3.5146
		0.5						1.6310	3.7619	1.6000	3.4823
		1						1.7780	3.7313	1.7391	3.4537
		0.2	0					1.5359	3.7820	1.5359	3.5091
			0.5					1.5359	3.7820	1.4505	3.4883
			1					1.5359	3.7820	1.4043	3.4655
			0.2	0.2				1.3833	3.2681	1.3545	2.9523
				0.5				1.4609	3.5286	1.4336	3.2337
				0.8				1.5359	3.7820	1.5098	3.5012
				0.8	0			1.5359	3.7820	1.5126	3.7739
					0.1			1.5359	3.7820	1.5113	3.6329
					1			1.5359	3.7820	1.4988	2.8276
					0.2	0		1.5359	3.9006	1.5111	3.6201
						0.15		1.5359	3.7208	1.5091	3.4398
						0.16		1.5359	3.7084	1.5090	3.4274
						0.1	0	1.5144	3.7880	1.4890	3.5069
							0.2	1.5573	3.7760	1.5306	3.4951
							0.3	1.5786	3.7700	1.5513	3.4899

Chapter 4

Conclusions

A brief description of previous knowledge is given in Chapter 1. It includes the definitions to some important fluids that are compressible, incompressible, real, ideal, steady , unsteady, laminar , turbulent, Newtonian and non-Newtonian fluids. It also included thr boundary layer flow. Some dimensionless parameters are also explained e.g Reynolds, Prandtl, Deborah and Nusselt number etc. At the end $bvp4c$ is also explained.

In Chapter 2, the impacts of variable characteristics and variable heat flux in a laminar flow of an incompressible fluid through an unsteady stretching surface embedded in a porous medium have been studied using numerical solutions. The $bvp4c$ is used to solve the numerically obtained similar ordinary differential equations. For various physical parameters, all values of parameters relating to the prevailing shear stress for fluid flow and heat transfer are arranged in the table. The $bvp4c$ was used to solve the numerically computed highly nonlinear ODEs that characterise our physical problem. We discovered that the local Nusselt number is highly influenced by the values of the S, ϵ, R, γ, M and α are influenced to a lesser extent. The rate of heat transmission was also shown to decrease when the viscosity and magnetic parameters increased. Furthermore, it was discovered that as the unsteadiness, radiation parameters and thermal conductivity rose, the rate of cooling for the surface is increased.

In chapter (3) comparison of constant and variable fluid properties with variable heat flux over a sheet for Maxwell fluid is done. bvp4c in MATLAB is used to solved

the obtained ordinary differential equations for both the cases constant fluid properties and variable fluid properties. For different physical parameters all the values of parameters corresponding to predominate the shear stress for fluid flow along with heat transfer are arranged in the table. The nonlinear ODEs obtained describe our physical problem were solved numerically by bvp4c in MATLAB. The notable findings of the problem are outlined below:

- For both cases skin-friction coefficient rises with the rising values of M, S, γ, ϵ and De.

- There is no decrease in the skin-friction coefficient for both cases. While the heat generation/absorption parameter values of skin-friction remains constant for Case A i.e. constant fluid properties are independent of heat generation/absorption parameter.

- For both the cases local Nusselt number increases with the increase in thermal radiation.

- For both the cases Nusselt number falls with the rise in magnetic parameter, γ, Deborah number and heat generation/absorption parameter. While viscosity parameter's value for Nusselt number remains constant for Case A.

- The temperature profile increases with the increase of α, De, γ, M, R and S_1. While it decreases with the increase of R, S and ϵ

- The velocity profile increases with the increase of ϵ, and R. While it decreases with the increase of α, S_1, S, γ, M and De.

- The Skin-friction coefficient and local Nusselt number values for Constant Fluid properties is greater than the values of Variable Fluid Properties.

Bibliography

[1] Stone, James M. "Astrophysical magnetohydrodynamics." Fluid Flows To Black Holes: A Tribute to S Chandrasekhar on His Birth Centenary, pp.177-190,2011.

[2] B. Jonathan, MHD: Astrophysical Contexts, Essential Fluid Dynamics for Scientists, Berlin, Germany, 2017.

[3] S. Bhattacharyya, A. Pal, A. Pal, and A. S. Gupta, "Heat transfer in the flow of a viscoelastic fluid over a stretching surface," Heat and Mass Transfer, vol. 34, no. 1, pp. 41-45, 1998.

[4] Char, Ming-I. "Heat transfer in a hydromagnetic flow over a stretching sheet." Warme-und Stoffubertragung 29.8, pp.495-500,1994.

[5] I. Pop and T.-Y. Na, "Unsteady flow past a stretching sheet," Mechanics Research Communications, vol. 23, no. 4, pp. 413-422, 1996.

[6] E. M. A. Elbashbeshy and M. A. A. Bazid, "Heat transfer over an unsteady stretching surface," Heat and Mass Transfer, vol. 41, no. 1, pp. 1-4, 2004.

[7] I.-C. Liu and H. I. Andersson, "Heat transfer in a liquid film on an unsteady stretching sheet," International Journal of Thermal Sciences, vol. 47, no. 6, pp. 766-772, 2008.

[8] M. A. El-Aziz, "Radiation effect on the flow and heat transfer over an unsteady stretching sheet," International Communications Heat and Mass Transfer, vol. 36, pp. 521-524, 2009.

[9] A. Ishak, R. Nazar, and I. Pop, "Heat transfer over an unsteady stretching permeable surface with prescribed wall temperature," Nonlinear Analysis: Real World Applications, vol. 10, no. 5, pp. 2909-2913, 2009.

[10] M. A. El-Aziz, "Flow and heat transfer over an unsteady stretching surface with Hall effect," Meccanica, vol. 45, pp. 97-109, 2010.

[11] B. K. Dutta, P. Roy, and A. S. Gupta, "Temperature field in flow over a stretching sheet with uniform heat flux," International Communications in Heat and Mass Transfer, vol. 12, no. 1, pp. 89-94, 1985.

[12] C.-L. Chang and Z.-Y. Lee, "Free convection on a vertical plate with uniform and constant heat flux in a thermally stratified micropolar fluid," Mechanics Research Communications, vol. 35, no. 6, pp. 421-427, 2008.

[13] C.-Y. Cheng, "Soret and Dufour effects on natural convection boundary layer flow over a vertical cone in a porous medium with constant wall heat and mass fluxes," International Communications in Heat and Mass Transfer, vol. 38, no. 1, pp. 44-48, 2011.

[14] I.-C. Liu, A. M. Megahed, and H.-H. Wang, "Heat transfer in a liquid film due to an unsteady stretching surface with variable heat flux," ASME Journal of Applied Mechanics, vol. 80, p. 41003, 2013.

[15] Rajagopal, K. R. "A note on unsteady unidirectional flows of a non-Newtonian fluid." International Journal of Non-Linear Mechanics 17.5-6,pp.369-373,1982.

[16] Wang, C. Y. "Liquid film on an unsteady stretching surface." Quarterly of applied Mathematics 48, no. 4, pp. 601-610, 1990.

[17] Tan W C, Xiao PWand Yu X M."A note on unsteady flows of a viscoelastic fluid with the fractional Maxwell model between two parallel plates." International Journal of Non-Linear Mechanics,vol.38,pp 645-650, 2003.

[18] Hayat, T., S. A. Shehzad, and A. Alsaedi. "Study on three-dimensional flow of Maxwell fluid over a stretching surface with convective boundary conditions." International Journal of Physical Sciences 7.5, pp.761-768, 2012 .

[19] Mukhopadhyay, Swati. "Heat transfer analysis of the unsteady flow of a Maxwell fluid over a stretching surface in the presence of a heat source/sink." Chinese Physics Letters 29.5,p. 054703.2012.

[20] Fetecau, Corina, M. Athar, and Constantin Fetecau. "Unsteady flow of a generalized Maxwell fluid with fractional derivative due to a constantly accelerating plate." Computers and Mathematics with Applications 57.4, pp.596-603,2009 .

[21] Megahed, Ahmed M. "Variable heat flux effect on magnetohydrodynamic flow and heat transfer over an unsteady stretching sheet in the presence of thermal radiation." Canadian Journal of Physics 92, no. 1, pp.86-91, 2014.

[22] Megahed, Ahmed M., et al. "Magnetohydrodynamic Fluid Flow due to an Unsteady Stretching Sheet with Thermal Radiation, Porous Medium, and Variable Heat Flux." Advances in Astronomy 2021,2021.

[23] Solving boundary value problems for ordinary differential equations in MATLAB with bvp4c, Tutorial Notes , pp.437-438, 2007.

[24] M. Mustafa, J.A. Khan, T. Hayat, A. Alsaedi, Sakiadis flow of Maxwell fluid considering magnetic field and convective boundary conditions, AIP. Adv. 5,p.027106,2015.

[25] S. Rashidi, J. A. Esfahani, and M. Maskaniyan, "Applications of magnetohydrodynamics in biological systems-a review on the numerical studies," Journal of Magnetism and Magnetic Materials, vol. 439, pp. 358-372, 2017.

[26] K. V. Prasad, K. Vajravelu, P. S. Datti, and B. T. Raju, "MHD flow and heat transfer in a power-law liquid film at a porous surface in the presence of thermal radiation," Journal of Applied Fluid Mechanics, vol. 6, pp. 385-395, 2013.

[27] L. J. Crane, "Flow past a stretching plate," Zeitschrift für angewandte Mathematik und Physik ZAMP, vol. 21, no. 4, pp. 645-647, 1970.

[28] J. Singh and R. Bajaj, "Parametric modulation in the Taylor-Couette ferrofluid flow," Fluid Dynamics Research, vol. 40, no. 10, pp. 737-752, 2008.

[29] J. Singh and R. Bajaj, "Dean instability in ferrofluids," Meccanica, vol. 51, no. 4, pp. 835-847, 2016.

[30] J. Singh, "A nonlinear shooting method and its application to nonlinear Rayleigh-Bénard convection," ISRN Mathematical Physics, vol. 2013, Article ID 650208, 2013.

[31] K. V. Prasad, D. Pal, and P. S. Datti, "MHD power-law fluid flow and heat transfer over a non-isothermal stretching sheet," Communications in Nonlinear Science and Numerical Simulation, vol. 14, no. 5, pp. 2178-2189, 2009.

[32] M. A. A. Mahmoud and A. M. Megahed, "MHD flow and heat transfer in a non-Newtonian liquid film over an unsteady stretching sheet with variable fluid properties," Canadian Journal of Physics, vol. 87, no. 10, pp. 1065-1071, 2009.

[33] B. S. Dandapat, B. Santra, and K. Vajravelu, "The effects of variable fluid properties and thermocapillarity on the flow of a thin film on an unsteady stretching

sheet," International Journal of Heat and Mass Transfer, vol. 50, no. 5-6, pp. 991-996, 2007.

[34] Abel, M. Subhas, Jagadish V. Tawade, and Mahantesh M. Nandeppanavar. "MHD flow and heat transfer for the upper-convected Maxwell fluid over a stretching sheet." Meccanica 47.2,pp.385-393, 2012.